


Role of triangle singularity in the decay process

$$D^0 \rightarrow \pi^+ \pi^- f_0(980), f_0 \rightarrow \pi^+ \pi^-$$

Dazhuang He, Yiling Xie, and Hao Sun^{*}*Institute of Theoretical Physics, School of Physics, Dalian University of Technology,
No. 2 Linggong Road, Dalian, Liaoning, 116024, People's Republic of China* (Received 6 March 2022; revised 23 April 2023; accepted 15 May 2023; published 30 May 2023)

We study the process $D^0 \rightarrow \pi^+ \pi^- f_0(980), f_0 \rightarrow \pi^+ \pi^-$ by introducing the triangle mechanism, in which $f_0(980)$ is considered to be dynamically generated from the meson-meson interaction. For the total contribution of this process, the contribution of the triangular loop formed by $K^* \bar{K} K$ particles could generate a triangular singularity of about 1418 MeV. We calculate the differential decay width of this process and show a narrow peak of about 980 MeV in the $\pi^+ \pi^-$ invariant mass distribution, which comes from f_0 decay. For the $M_{\text{inv}}(\pi f_0)$ invariant mass distribution, we obtain a finite peak at 1418 MeV, which is consistent with the triangle singularity.

DOI: [10.1103/PhysRevD.107.094040](https://doi.org/10.1103/PhysRevD.107.094040)**I. INTRODUCTION**

Triangle diagrams give the same good descriptions in the hadron physics, but of particular concern are those that lead to triangle singularities (TS) in amplitude [1–4]. Triangle singularities were introduced by Landau [5,6]. Nowadays, a large amount of peaks observed in high-energy experiments are considered to be caused by triangle singularities, especially the processes involving heavy quarks. With the development of experiments, triangle singularities play an increasingly important role in hadron physics. The picture of the triangle mechanism can be summarized as follows: the initial particle A decays into two internal particles 1 and 2 flying back-to-back, particle 2 decays into internal particle 3 and external particle B , the former moves in the same direction as particle 1, and the two internal particles 1 and 3 rescatter to form an external particle C . According to the Coleman-Norton theorem [4], the generation of triangle singularity depends on whether the above process is a classical process and whether all three internal particles are simultaneously placed on-shell and collinear in the rest frame of the decay particle [5]. In reality, the internal particles have finite widths and result in the transformation of triangle singularities to finite peaks which can be observed in experiments.

In Ref. [7], the triangle singularity was introduced to explain $J/\psi \rightarrow \gamma \eta(1405/1475) \rightarrow \gamma \pi^0 f_0(980) \rightarrow \gamma 3\pi$

experiment data, and gave some good conclusions to explain the $f_0 - a_0$ mixing and the relation between $\eta(1405/1475)$. Soon after, some literature were published to analyze the important role of triangle singularity in the process $\eta(1405) \rightarrow f_0(980) \pi^0$ [8–11]. Meanwhile, in order to further solve the issue of $f_0(980) - a_0(980)$ mixing and isospin breaking, the triangle mechanism in different processes that contain $f_0 - a_0$ mixing has been researched [12–18]. In Ref. [19], the production of $f_0(980)$ in semilepton decay process $\tau^- \rightarrow \nu_\tau \pi^- f_0(980)$ has been studied through a $K^* K^+ K^-$ triangle loop which produces a singularity located at 1418 MeV in the πf_0 invariant mass distribution. Applying triangle mechanism to $f_1(1285) \rightarrow \pi_0 a_0(980)$ and $f_1(1285) \rightarrow \pi_0 f_0(980)$ processes and considering all three resonances as dynamically generated states, authors in Ref. [12] obtained the branching fractions which are consistent with the experiments. Especially in Ref. [14], authors found the two nonresonant peaks at 2850 MeV in the invariant mass of πD_{s0} pairs and around the 3000 MeV in the invariant mass of πD_{s1}^+ pairs, which are associated with the kinematical triangle singularities. By adjusting the values of ϵ and K^* width, it shows the peak's developmental behavior of the real and imaginary parts of the loop function.

Recently, the authors in Ref. [20] proposed the triangle singularity close to the $\bar{K}d$ threshold for the first time in the $p \Sigma^- \rightarrow K^- d$ and $K^- d \rightarrow p \Sigma^-$ processes. In Ref. [21], the processes $D_s^+ \rightarrow a_0(980) \rho$ and $a_0(980) \omega$ including a $\pi^+ \pi^+ \eta$ loop have been researched. Further, for the $\psi(2s) \rightarrow \pi^+ \pi^- K^+ K^-$ process, the authors in Ref. [22] introduced a moving triangle singularity in the range of 1.158 to 1.181 GeV. In addition, a lot of other research has been done on the triangle mechanism [23–50].

^{*}haosun@dlut.edu.cn

Published by the American Physical Society under the terms of the [Creative Commons Attribution 4.0 International license](https://creativecommons.org/licenses/by/4.0/). Further distribution of this work must maintain attribution to the author(s) and the published article's title, journal citation, and DOI. Funded by SCOAP³.

In this paper, following the procedure in Refs. [14,28], we study $D^0 \rightarrow \pi^+\pi^-f_0$ and $D^0 \rightarrow \pi^+\pi^-f_0$, $f_0 \rightarrow \pi^+\pi^-$, decay processes by introducing triangle mechanism. The amplitude for the production of $f_0(980)$ could be obtained by chiral unitary approach, which f_0 is considered as dynamically generated from the meson-meson interaction [51–53]. We consider the main contributions of $K^{*0}K^+K^-$ triangle loop as well as the contributions that come from intermediate state $a_1^+(1260)$. Although the traditional Feynman parametrization and dispersion relation methods could be used to calculate the loop integral to obtain the triangular amplitude, the authors in Refs. [54,55] put forward a simple formula to judge whether the triangular singularity exist, such formula is derived by performing the residue theorem on the loop function, and the poles of the spatial integral are then analyzed. In order to obtain the total amplitude of this process, some coupling strength for different D^0 decay processes needs to be calculated by fitting to corresponding experimental data.

The structure of this paper is as follows. In Sec. II, the detailed pictures of $D^0 \rightarrow \pi^+\pi^-f_0(980)$, $f_0 \rightarrow \pi^+\pi^-$ decay process and interaction vertices including D^0 have been depicted. We calculate the coupling strength of the $D^0K^{*0}K^-\pi^+$ and $D^0a_1^+\pi^-$ vertices by fitting the corresponding experiments. Then, we give the derivation details and formalism for the calculation of $D^0 \rightarrow \pi^+\pi^-f_0(980)$, $f_0 \rightarrow \pi^+\pi^-$ decay that contains the triangle mechanism, where f_0 is considered as the dynamically generated states. Moreover, we give the expressions of the amplitudes for the corresponding Feynman diagrams. In Sec. III, the numerical results for differential distribution of decay width as a function of the invariant masses have been shown. Finally, a brief summary is given in Sec. IV.

II. FORMALISM

In this section, we show that a peak around 1.42 GeV in the $M_{\text{inv}}(\pi f_0)$ invariant mass distribution will be produced in the $D^0 \rightarrow \pi^+\pi^-f_0(980)$ and $D^0 \rightarrow \pi^+\pi^-f_0(980)$, $f_0 \rightarrow \pi^+\pi^-$ decay processes by triangle singularity. The total Feynman diagrams contributing to this process, which include the $\bar{K}^{*0}(K^{*0})K^+K^-$ and $K^{*+}\bar{K}^0K^0$ triangle loops, have been depicted in Fig. 1. In order to determine the interaction strength of the first decay vertices of Fig. 1, such as $D^0 \rightarrow \pi^+K^{*0}K^-$ and $D^0 \rightarrow a_1^+\pi^-$, the access to the corresponding decay width is essential. From the PDG [56], for the first vertex of $D^0 \rightarrow \pi K^* K$ process Figs. 1(a) and 1(d), there is only the production channel of $\pi^\mp K^{*0} K^\pm$ pair. Because the 3rd component of isospin obeys the conservation law, only the Figs. 1(a) and 1(d) will contribute to the total amplitude for the first $D^0 \rightarrow \pi K^* K$ vertex. There is the similar situation for other subfigures of Fig. 1, but Ref. [57] gives the branching fractions of $a_1^+\pi^-$ and $a_1^-\pi^+$ productions, which the former is about two orders of magnitude larger than the latter. Thus, for the vertices of $D^0 \rightarrow a_1^\pm \pi^\mp$ processes, we neglect the contribution from the $D^0 a_1^-\pi^+$ vertex. Another important point is that the a_1 from the D^0 decay will be considered as dynamically generated in a two coupled channel problem with building blocks $\rho\pi$ and \bar{K}^*K [15,57]. Thus, the a_1 could decay to $f_0\pi$ by the $\bar{K}^*K\bar{K}$ and $\rho\pi\pi$ triangle loop as Refs. [15,18,57,58]. Because the width of ρ meson is very broad, the contributions from the $\rho\pi\pi$ triangle loop are neglected [45,55]. In the following, we will take Figs. 1(a) and 1(d) as examples to perform the calculation and discussion. From Fig. 1(a), we can see that the D^0 decays to $\pi^+K^{*0}K^-$ first, then the K^{*0} decays to the π^-K^+ . Since the K^+ and K^- move in the same direction, and the former

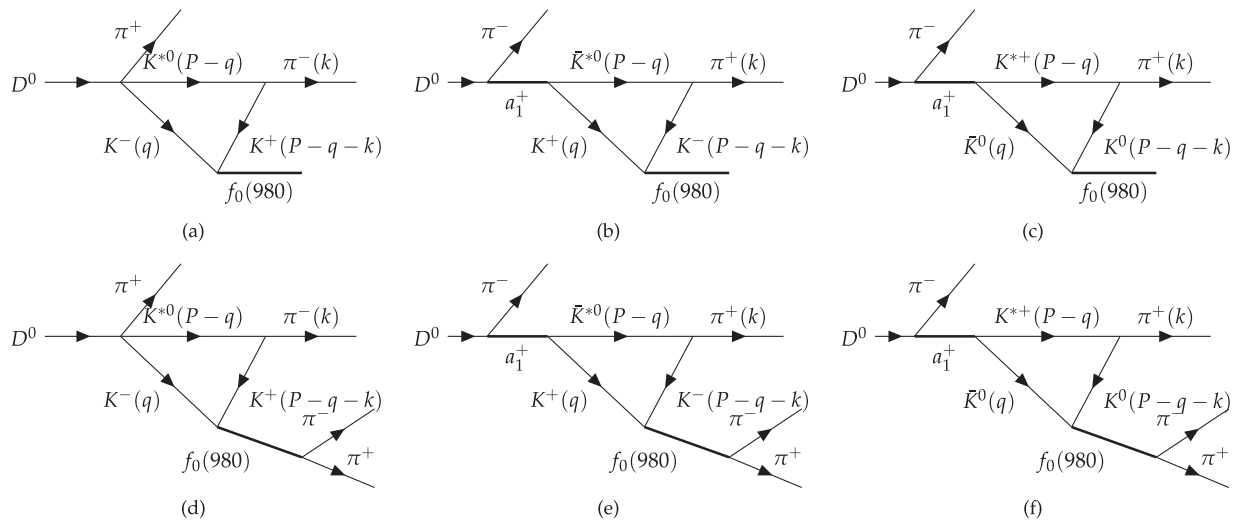


FIG. 1. The total Feynman diagrams contributing to $D^0 \rightarrow \pi^+\pi^-f_0(980)$ and $D^0 \rightarrow \pi^+\pi^-f_0(980)$, $f_0(980) \rightarrow \pi^+\pi^-$ decay processes involving intermediate state a_1 and $\bar{K}^*K\bar{K}$ triangle loop.

is faster than the latter, the K^+K^- rescattered to form $f_0(980)$. Meanwhile, f_0 could be considered as the dynamically generated states of the $\pi^+\pi^-$, K^+K^- , $\pi^0\pi^0$, $K^0\bar{K}^0$, and $\eta\eta$ in S -wave within the chiral unitary approach [51–53].

It is worthy to note that there is a triangle singularity for the $K^{*0}K^+K^-$ triangle loop in Fig. 1 when we take value of the $f_0(980)$ mass just above the K^+K^- threshold, in other words, the mass m_{f_0} must meet the condition for triangle singularity [54,55]

$$m_{f_0}^2 \in \left[(2m_K)^2, \frac{(m_K + m_{K^{*0}})(m_K m_{K^{*0}} + m_K^2) - m_K m_\pi}{m_{K^{*0}}} \right]. \quad (1)$$

In order to get the triangle singularity, it is straightforward to use the following condition

$$\lim_{\epsilon \rightarrow 0} (q_+^{\text{on}} - q_-^{\text{a}}) = 0, \quad \text{and} \quad q_+^{\text{on}} = \frac{\lambda^{\frac{1}{2}}(M_{\text{inv}}^2(\pi f_0), M_{K^+}^2, M_{K^{*0}}^2)}{2M_{\text{inv}}(\pi f_0)}, \quad (2)$$

where q_+^{on} denotes the on shell three momentum of K^- in the center-of-mass frame (COM) of $K^{*0}K^-$, $M_{\text{inv}}(\pi f_0)$ is the invariant-mass of $K^{*0}K^-$ system, and $\lambda(x, y, z) = x^2 + y^2 + z^2 - 2xy - 2yz - 2xz$ is the Kahlen function. Meanwhile, q_-^{a} is given by

$$q_-^{\text{a}} = \gamma(\nu E_{K^+}^* - p_{K^+}^*) - i\epsilon, \quad (3)$$

with definitions

$$\nu = \frac{k}{E_{f_0}}, \quad \gamma = \frac{1}{\sqrt{1-\nu^2}} = \frac{E_{f_0}}{m_{f_0}},$$

$$E_{K^+}^* = \frac{m_{f_0}^2 + m_{K^+}^2 - m_{K^*}^2}{2m_{f_0}}, \quad p_{K^+}^* = \frac{\lambda^{\frac{1}{2}}(m_{f_0}^2, M_{K^-}^2, M_{K^+}^2)}{2m_{f_0}}, \quad (4)$$

where $E_{K^+}^*$ and $p_{K^+}^*$ are the energy and momentum of the K^+ meson in the COM frame of the K^+K^- system, ν and γ are the velocity of the K^+K^- system and Lorentz boost factor, respectively. When Eq. (2) is established, on the one hand, it means that all particles in the triangle loop are on-shell, the K^- and $f_0(980)$ move in the same direction in the rest frame of $f_0(980)$ and COM frame of $\pi f_0(980)$, respectively. Meantime, in order that the K^+ and K^- in the triangle loop could rescatter to form the $f_0(980)$ in a classical picture, it is required that the momentum of K^- in the COM frame of πf_0 is smaller than that of K^+ in the rest frame of the decay particle, which is derived from the $K^{*0} \rightarrow K^+\pi^-$ decay. On the other hand, in mathematics, Eq. (2) represents that q_-^{a} and q_+^{on} are the singularities of

triangle loop function in the upper and lower half of the complex- q plane, respectively, and the integration path of loop function Eq. (22) is pinched between q_-^{a} and q_+^{on} in the same position of the real axis. In addition,

$$E_{f_0} = \frac{M_{\text{inv}}^2(\pi f_0) + m_{f_0}^2 - m_{\pi^+}^2}{2M_{\text{inv}}(\pi f_0)},$$

$$k = \frac{\lambda^{\frac{1}{2}}(M_{\text{inv}}^2(\pi f_0), m_{f_0}^2, m_{\pi^+}^2)}{2M_{\text{inv}}}. \quad (5)$$

Now, we can obtain a triangle singularity around 1418 MeV in the $M_{\text{inv}}(\pi f_0)$ invariant mass distribution by using Eq. (2). Further, when the complex mass of K^{*0} with $m_{K^{*0}}' = m_{K^{*0}} - i\Gamma_{K^{*0}}/2$, $\Gamma_{K^{*0}} = 50$ MeV is used in Eq. (2), it leads to a complex triangle singularity near $1418 - i29.7$ MeV.

A. The process of $D^0 \rightarrow K^{*0}\pi K$

Before calculating the amplitudes of Fig. 1(a), the amplitudes of $D^0 \rightarrow \pi^+ K^{*0} K^-$ decay processes need to be established to determine the vertex couplings strength. The pictures of decay processes at the quark level as shown in Fig. 2, which only includes the $\pi^+ K^{*0} K^-$ final state. Taking Fig. 2 as an example, the first part is that the $\bar{d}u$ and $d\bar{u}$ quark pairs could be produced via an external emission of a W boson, where two vertices cdW and $u\bar{d}W$ included by the weak decay are Cabibbo-suppressed and Cabibbo-favored, respectively. In the next step, the $\bar{d}u$ quark-antiquark pair hadronizes and produces a π^+ meson. At the same time, the remaining $d\bar{u}$ and $s\bar{s}$ quark-antiquark pairs, selected from the vacuum $\bar{q}q(\bar{u}u + \bar{d}d + \bar{s}s)$ state, combine to form the $K^{*0}K^-$ vector-pseudoscalar mesons pair.

In order to conserve angular momentum, the coupling vertex of Fig. 2 can be calculated via the P -wave interaction. Following the construction of vertex interactions in Refs. [16,28], we take

$$-it_{D^0 \rightarrow K^{*0}\pi^+K^-} = -iC\vec{\epsilon}_{K^{*0}} \cdot \vec{p}_{\pi^+}, \quad (6)$$

where $\vec{\epsilon}_{K^{*0}}$ and \vec{p}_{π^+} are the polarization vector of K^{*0} and momentum of the π^+ , respectively. The C presents the coupling strength of this vertex, the analytical expression

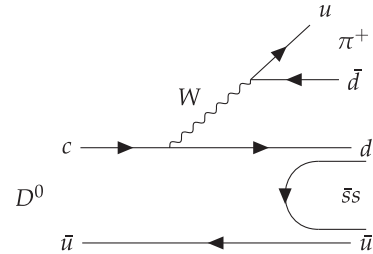


FIG. 2. The $D^0 \rightarrow \pi^+ K^{*0} K^-$ decay process at the quark level.

and numerical results will be given below. From Eq. (2), we have obtained the triangle singularity around 1.42 GeV, thus the momentum of K^{*0} is approximately 135.66 MeV in the $\pi^- f_0$ rest frame, which is smaller than the K^{*0} mass 895.81 MeV. For this reason, we can safely ignore the time-component ϵ^0 of the K^{*0} polarization vector, so the following form of polarization sum is taken

$$\sum_{\mu,\nu} \epsilon_{K^{*0}\mu} \epsilon_{K^{*0}\nu} \sim \sum_{i,j} \epsilon_{K^{*0}i} \epsilon_{K^{*0}j} = \delta_{ij}; \quad \mu = i, \quad (7)$$

$$\mu = j; \quad i, j = 1, 2, 3.$$

From the PDG [56], the partial decay branching ratio are $\Gamma(D^0 \rightarrow K^{*0} K^\mp \pi^\pm, K^{*0} \rightarrow K^\pm \pi^\mp) / \Gamma(K^+ K^- \pi^+ \pi^-) = 11 \pm 2 \pm 1\%$ and $\text{Br}(K^+ K^- \pi^+ \pi^-) = (2.45 \pm 0.11) \times 10^{-3}$. Considering the $\text{Br}(K^{*0} \rightarrow K\pi) \sim 100\%$, we can get $\text{Br}(D^0 \rightarrow K^{*0} K^- \pi^+) = \frac{3}{2} \text{Br}(D^0 \rightarrow K^{*0} K^- \pi^+, K^{*0} \rightarrow K^+ \pi^-)$. Meanwhile, the decay width of $D^0 \rightarrow \pi^+ K^{*0} K^-$ process is given by

$$\Gamma_{D^0 \rightarrow \pi^+ K^{*0} K^-} = \int dM_{\text{inv}}(K^{*0} K^-) \frac{1}{(2\pi)^3} \frac{|\vec{p}'_{K^-}| |\vec{p}_{\pi^+}|}{4m_{D^0}^2} \times \sum_{\text{pol}} |t_{D^0 \rightarrow \pi^+ K^{*0} K^-}|^2, \quad (8)$$

where $M_{\text{inv}}(K^{*0} K^-)$ is the invariant mass of the $K^{*0} K^-$ system. The $\vec{p}'_{K^-}, \vec{p}_{\pi^+}$ are three momentum of the K^- in the $K^{*0} K^-$ COM frame and that of the π^+ in the D^0 rest frame, respectively. They are given by

$$|\vec{p}'_{K^-}| = \frac{\lambda^{\frac{1}{2}}(M_{\text{inv}}^2(K^{*0} K^-), M_{K^-}^2, M_{K^{*0}}^2)}{2M_{\text{inv}}(K^{*0} K^-)},$$

$$|\vec{p}_{\pi^+}| = \frac{\lambda^{\frac{1}{2}}(M_{D^0}^2, M_{\text{inv}}^2(K^{*0} K^-), M_{\pi^+}^2)}{2M_{D^0}}. \quad (9)$$

After squaring the amplitude $t_{D^0 \rightarrow \pi^+ K^{*0} K^-}$ and employing the polarization sum Eq. (7), we get

$$\sum_{\text{pol}} |t_{D^0 \rightarrow \pi^+ K^{*0} K^-}|^2 = C^2 |\vec{p}'_{\pi^+}|^2, \quad (10)$$

where the \vec{p}'_{π^+} is the three momentum of the π^+ in the $K^{*0} K^-$ COM frame

$$|\vec{p}'_{\pi^+}| = \frac{\lambda^{\frac{1}{2}}(M_{D^0}^2, M_{\text{inv}}^2(K^{*0} K^-), M_{\pi^+}^2)}{2M_{\text{inv}}(K^{*0} K^-)}. \quad (11)$$

Finally, combining the Eqs. (8) and (10), C^2/Γ_{D^0} is given by

$$\frac{C^2}{\Gamma_{D^0}} = \frac{\text{Br}(D^0 \rightarrow \pi^+ K^{*0} K^-)}{\int dM_{\text{inv}}(K^{*0} K^-) \frac{1}{(2\pi)^3} \frac{|\vec{p}'_{K^-}| |\vec{p}_{\pi^+}|}{4m_{D^0}^2} |\vec{p}'_{\pi^+}|^2} \sim 5.69516 \times 10^{-7} \text{ MeV}^{-1}. \quad (12)$$

B. The processes $D^0 \rightarrow \pi^+ \pi^- f_0(980)$ and $D^0 \rightarrow \pi^+ \pi^- f_0(980), f_0(980) \rightarrow \pi^+ \pi^-$

For the Feynman diagrams of Fig. 1(a) process, according to the Feynman rules, we have the following amplitude form

$$-it_{D^0 \rightarrow \pi^+ \pi^- f_0} = i \sum_{\text{pol}} \int \frac{d^4 q}{(2\pi)^4} \frac{it_{D^0 \rightarrow \pi^+ K^{*0} K^-}}{q^2 - m_K^2 + i\epsilon} \times \frac{it_{K^{*0} K^+ \pi^-}}{(P-q)^2 - m_{K^*}^2 + i\epsilon} \times \frac{it_{K^+ K^- f_0}}{(P-q-k)^2 - m_K^2 + i\epsilon}, \quad (13)$$

in the COM frame of $\pi^- f_0$ where the π^- comes from the K^{*0} decay. It can be seen from Eq. (13) that in order to obtain full amplitude, the $t_{D^0 \rightarrow \pi^+ K^{*0} K^-}, t_{K^{*0} K^+ \pi^-}$ and $t_{K^+ K^- f_0}$ need to be calculated. And, the $t_{D^0 \rightarrow \pi^+ K^{*0} K^-}$ has been obtained in Eqs. (6) and (12).

In order to calculate the $t_{K^{*0} K^+ \pi^-}$, we need to employ the chiral invariant Lagrangian with the local hidden symmetry [59,60], which is given by

$$\mathcal{L}_{\text{VPP}} = -ig \langle V^\mu [P, \partial_\mu P] \rangle, \quad (14)$$

where the brackets $\langle \dots \rangle$ represent SU(3) trace, and coupling constant $g = m_V/2f_\pi$ in the local hidden gauge, with $m_V = 800$ MeV and $f_\pi = 93$ MeV. The P and V^μ stand for the pseudoscalar and vector mesons octet, respectively, which are given by

$$P = \begin{pmatrix} \frac{\pi^0}{\sqrt{2}} + \frac{\eta_8}{\sqrt{6}} & \pi^+ & K^+ \\ \pi^- & -\frac{\pi^0}{\sqrt{2}} + \frac{\eta_8}{\sqrt{6}} & K^0 \\ K^- & \bar{K}^0 & -\frac{2}{\sqrt{6}} \eta_8 \end{pmatrix},$$

$$V = \begin{pmatrix} \frac{\rho^0}{\sqrt{2}} + \frac{\omega}{\sqrt{2}} & \rho^+ & K^{*+} \\ \rho^- & -\frac{\rho^0}{\sqrt{2}} + \frac{\omega}{\sqrt{2}} & K^{*0} \\ K^{*-} & \bar{K}^{*0} & \phi \end{pmatrix}. \quad (15)$$

Then, the amplitude of K^{*0} decay is written as

$$-it_{K^{*0} K^+ \pi^-} = -ig \vec{\epsilon}_{K^{*0}} \cdot (\vec{p}'_{\pi^-} - \vec{p}'_{K^+}). \quad (16)$$

Similarly to the calculations of Eq. (10), the zero component of polarization vector in Eq. (16) is omitted, and the polarization sum Eq. (7) is also used here. The \vec{p}'_{π^-} and \vec{p}'_{K^+} are the momenta of the π^- and K^+ in the COM frame of πf_0 , respectively, and the former is given by

$$|\vec{p}'_{\pi^-}| = |\vec{k}| = \frac{\lambda^{\frac{1}{2}}(M_{\text{inv}}^2(\pi f_0), M_{\pi^-}^2, M_{f_0}^2)}{2M_{\text{inv}}(\pi f_0)}. \quad (17)$$

$$t_{K^+K^-f_0} = g_{K^+K^-f_0}. \quad (18)$$

Finally, the $t_{K^+K^-f_0}$ need to be provided, in which f_0 could be considered as the dynamically generated state. Thus the amplitude is simply written as

Now, by substituting Eqs. (6), (16), and (18) into Eq. (13), we can get

$$t_{D^0 \rightarrow \pi^+ \pi^- f_0} = ig_{K^+K^-f_0} g_C \sum_{\text{pol}} \int \frac{d^4 q}{(2\pi)^4} \frac{\vec{\epsilon}_{K^*} \cdot \vec{p}'_{\pi^+}}{q^2 - m_K^2 + i\epsilon} \frac{\vec{\epsilon}_{K^*} \cdot (\vec{p}'_{\pi^-} - \vec{p}'_{K^+})}{(P-q)^2 - m_{K^*}^2 + i\epsilon} \frac{1}{(P-q-k)^2 - m_K^2 + i\epsilon}, \quad (19)$$

where \vec{p}'_{π^-} could be obtained from Eq. (17) and the \vec{p}'_{π^+} is the momentum of the π^+ in the COM frame of πf_0 , which comes from the D^0 decay. We have

$$|\vec{p}'_{\pi^+}| = \frac{\lambda^{\frac{1}{2}}(M_{D^0}^2, M_{\text{inv}}^2(\pi f_0), M_{\pi^+}^2)}{2M_{\text{inv}}(\pi f_0)}. \quad (20)$$

The Eq. (7) could be employed to perform polarization sum of Eq. (19), which gives

$$t_{D^0 \rightarrow \pi^+ \pi^- f_0} = -ig_{K^+K^-f_0} g_C \int \frac{d^4 q}{(2\pi)^4} \frac{1}{q^2 - m_K^2 + i\epsilon} \frac{\vec{p}'_{\pi^+} \cdot (2\vec{k} + \vec{q})}{(P-q)^2 - m_{K^*}^2 + i\epsilon} \frac{1}{(P-q-k)^2 - m_K^2 + i\epsilon}, \quad (21)$$

where $P = (M_{\text{inv}}, 0, 0, 0)$ and $\vec{p}'_{\pi^-} - \vec{p}'_{K^+} = \vec{k} - (-\vec{k} - \vec{q}) = 2\vec{k} + \vec{q}$. We define expression t_T as

$$t_T = i \int \frac{d^4 q}{(2\pi)^4} \vec{p}'_{\pi^+} \cdot (2\vec{k} + \vec{q}) \frac{1}{q^2 - m_K^2 + i\epsilon} \frac{1}{(P-q)^2 - m_{K^*}^2 + i\epsilon} \frac{1}{(P-q-k)^2 - m_K^2 + i\epsilon}. \quad (22)$$

For the K^{*0} propagator in the t_T , we can ignore the part of negative energy as Refs. [12,54,55]. After performing analytically integration Eq. (22) in dq^0 by using residue theorem, we can use the following formula

$$\int d^3 q \vec{q} f(\vec{q}, \vec{k}) = \vec{k}_i \int d^3 q \frac{\vec{q} \cdot \vec{k}}{|\vec{k}|^2} f(\vec{q}, \vec{k}). \quad (23)$$

Now, Eq. (22) reduces to

$$t_T = \vec{p}'_{\pi^+} \cdot \vec{k} \int \frac{d^3 q}{(2\pi)^3} \frac{1}{8\omega_{K^-}(\vec{q}) E_{K^*}(\vec{q}) E_{K^+}(\vec{k} + \vec{q}) k^0 - E_{K^*}(\vec{q}) - E_{K^+}(\vec{k} + \vec{q}) P^0 + \omega_{K^-}(\vec{q}) + E_{K^+}(\vec{k} + \vec{q}) - k^0} \times \frac{2P^0 \omega_{K^-}(\vec{q}) + 2k^0 E_{K^+}(\vec{k} + \vec{q}) - 2[\omega_{K^-}(\vec{q}) + E_{K^+}(\vec{k} + \vec{q})][\omega_{K^-}(\vec{q}) + E_{K^*}(\vec{q}) + E_{K^+}(\vec{k} + \vec{q})]}{[P^0 - \omega_{K^-}(\vec{q}) - E_{K^+}(\vec{k} + \vec{q}) - k^0 + i\epsilon][P^0 - \omega_{K^-}(\vec{q}) - E_{K^*}(\vec{q}) + i\epsilon]} \left(2 + \frac{\vec{q} \cdot \vec{k}}{|\vec{k}|^2}\right), \quad (24)$$

$$= \vec{p}'_{\pi^+} \cdot \vec{k} \times \tilde{t}_T,$$

where $\omega_{K^-}(\vec{q}) = \sqrt{m_{K^-}^2 + \vec{q}^2}$, $E_{K^{*0}}(\vec{q}) = \sqrt{m_{K^{*0}}^2 + \vec{q}^2}$, $E_{K^+}(\vec{q} + \vec{k}) = \sqrt{m_{K^+}^2 + (\vec{k} + \vec{q})^2}$ and $k^0 = \sqrt{m_{\pi^-}^2 + \vec{k}^2}$ are the energy of K^- , K^{*0} , K^+ and π^- in the COM frame of πf_0 system, respectively. While $P^0 = M_{\text{inv}}(\pi f_0)$ is the invariant mass of the πf_0 system. The $|\vec{q}|$ integral in the Eq. (24) is regulated by cutoff scheme, $\theta(q_{\text{max}} - |q^*|)$,

where $|q^*|$ is the momentum of K^- in the f_0 rest frame. The $q_{\text{max}} = 600$ MeV in the f_0 rest frame was obtained in the chiral unitary approach by fitting experimental data. In the following calculation, we need to add the width for K^{*0} with the replacement of $E_{K^{*0}}$ by $E_{K^{*0}} - i\Gamma_{K^{*0}}/2$ in the denominator of Eq. (24).

Finally, for the three body decay process as depicted in Fig. 1(a), the mass distribution of differential width could be written as

$$\frac{d\Gamma'}{dM_{\text{inv}}(\pi f_0)} = \frac{1}{3} \frac{1}{(2\pi)^3} \frac{C^2 g_{K^+K^-f_0}^2 g^2}{4m_{D^0}^2} |\vec{p}_{\pi^+}| |\vec{k}| |t_T|^2, \quad (25)$$

where the 1/3 in Eq. (25) originates from the integrand of phase-space angle in $\vec{p}'_{\pi^+} \cdot \vec{k} = |\vec{p}'_{\pi^+}| |\vec{k}| \cos\theta$,

and the \vec{p}_{π^+} is the momentum of the π^+ in the D^0 rest frame

$$|\vec{p}_{\pi^+}| = \frac{\lambda^{\frac{1}{2}}(m_{D^0}^2, M_{\pi^+}^2, M_{\text{inv}}^2(\pi^- f_0))}{2m_{D^0}}. \quad (26)$$

At the same time, the other Feynman diagrams contributions Figs. 1(b) and 1(c) were considered to calculate the differential decay width. Here we give the amplitude expressions (t) for the Figs. 1(a)–1(c) directly

$$\begin{aligned} t^a &= -C(C_2^a g) \vec{p}'_{\pi^+} \cdot \vec{k} \times \tilde{t}_T(m_{K^{*0}}, m_{K^-}, m_{K^+})(C_3^a g_{\bar{K}Kf_0}), \\ t^b &= -C' \frac{1}{M_{\text{inv}}^2(\pi f_0) - m_{a_1}^2 + im_{a_1}\Gamma_{a_1}} (C_1^b g_{\bar{K}^*K a_1})(C_2^b g) \vec{p}'_{\pi^-} \cdot \vec{k} \times \tilde{t}_T(m_{\bar{K}^{*0}}, m_{K^+}, m_{K^-})(C_3^b g_{\bar{K}Kf_0}), \\ t^c &= -C' \frac{1}{M_{\text{inv}}^2(\pi f_0) - m_{a_1}^2 + im_{a_1}\Gamma_{a_1}} (C_1^c g_{\bar{K}^*K a_1})(C_2^c g) \vec{p}'_{\pi^-} \cdot \vec{k} \times \tilde{t}_T(m_{K^{*+}}, m_{\bar{K}^0}, m_{K^0})(C_3^c g_{\bar{K}Kf_0}). \end{aligned} \quad (27)$$

From Refs. [7,9,15], the values of factor C_i^j have been shown in Table I. We have $g_{\bar{K}Kf_0} = g_{K^+K^-f_0} = -g_{\bar{K}^0K^0f_0}$ for the coupling between $\bar{K}K$ and f_0 in isospin base. The value of coupling $g_{\bar{K}^*K a_1}$ in isospin base has been give in Ref. [61]

$$g_{\bar{K}^*K a_1} = (1872 - i1486) \text{ MeV}. \quad (28)$$

Meanwhile, the coupling between a_1^+ and the combination with $I = 1$, $C = +$ and $G = -$ of the \bar{K}^*K pair is represented by the state

$$\frac{1}{\sqrt{2}} (\bar{K}^*K - K^*\bar{K}) = \frac{1}{\sqrt{2}} (\bar{K}^{*0}K^+ - K^{*+}\bar{K}^0). \quad (29)$$

The C' in the $t^{(b)(c)}$ stand for the effective coupling strength of $D^0 \rightarrow a_1^+ \pi^-$ vertices. In the derivation of C' , combining $\text{Br}(D^0 \rightarrow a_1^+(1260), a_1 \rightarrow 2\pi^+ \pi^-) = (4.52 \pm 0.31) \times 10^{-3}$ from PDG and Refs. [57,62], we take the branch ratio as $\text{Br}(D^0 \rightarrow a_1^+ \pi^-) = (4.1 \pm 0.4) \times 10^{-3}$. For the propagator of a_1 in Eq. (27), we take parameters of a_1 as $m_{a_1} = 1230$ MeV and $\Gamma_{a_1} = 425$ MeV, coming from the use of Ref. [23].

Meanwhile, we further consider that the $f_0(980)$ decay to the $\pi^+ \pi^-$ final state, as depicted in Fig. 1(d). In order to write amplitude of $D^0 \rightarrow \pi^+ \pi^- f_0(980)$, $f_0 \rightarrow \pi^+ \pi^-$ process, following Refs. [28,34], we only need to replace the couplings $C_3^a g_{\bar{K}Kf_0}$ or $g_{K^+K^-f_0}$ in Eqs. (25) and (27) by the transition amplitude $t_{K^+K^- \rightarrow \pi^+ \pi^-}$. The amplitude $t_{K^+K^- \rightarrow \pi^+ \pi^-}$ is obtained by solving the coupled channels Bethe-Salpeter (BS) equation in the chiral unitary approach, in which f_0

appears as dynamically generated state. The BS equation is given by

$$T = [1 - VG]^{-1} V, \quad (30)$$

where the V and G are the interaction potential and meson loop function respectively, which have been calculated in Ref. [51]. The meson loop function G is regulated by a cutoff $q_{\text{max}} = 600$ MeV. Finally, the double differential distribution for $D^0 \rightarrow \pi^+ \pi^- f_0(980)$, $f_0 \rightarrow \pi^+ \pi^-$ decay process is written as

$$\begin{aligned} & \frac{d^2\Gamma'}{dM_{\text{inv}}(\pi f_0) dM_{\text{inv}}(\pi^+ \pi^-)} \\ &= \frac{g^2 C^2}{(2\pi)^5} \frac{|\vec{p}_{\pi^+}| |\vec{q}_{\pi^-}| |\vec{k}|}{4m_{D^0}^2} |t_T|^2 \cdot |t_{K^+K^- \rightarrow \pi^+ \pi^-}|^2. \end{aligned} \quad (31)$$

TABLE I. Coefficients entering the evaluation of amplitudes in Eqs. (27) and (32). The C_2 have a minus sign compared with Ref. [15], this is because that we taken the $\vec{p}'_{\pi^-} - \vec{p}'_{K^+} = 2\vec{k} + \vec{q}$ form used in Refs. [14] for the VPP vertex instead of $P - 2\vec{k} - \vec{q}$ in Ref. [15].

Diagram	C_1	C_2	C_3
Figure 1(a)	...	1	1
Figure 1(b)	$\frac{1}{\sqrt{2}}$	1	1
Figure 1(c)	$-\frac{1}{\sqrt{2}}$	-1	-1

Similar to Eq. (27), the amplitudes expressions of Figs. 1(d)–1(f) have

$$\begin{aligned}
 t^d &= -C(C_2^a g) \vec{p}'_{\pi^+} \cdot \vec{k} \times \tilde{t}_T(m_{K^{*0}}, m_{K^-}, m_{K^+})(t_{K^+ K^- \rightarrow \pi^+ \pi^-}), \\
 t^e &= -C' \frac{1}{M_{\text{inv}}^2(\pi f_0) - m_{a_1}^2 + im_{a_1} \Gamma_{a_1}} (C_1^b g_{\bar{K}^* K a_1})(C_2^b g) \vec{p}'_{\pi^-} \cdot \vec{k} \times \tilde{t}_T(m_{\bar{K}^{*0}}, m_{K^+}, m_{K^-})(t_{K^+ K^- \rightarrow \pi^+ \pi^-}), \\
 t^f &= -C' \frac{1}{M_{\text{inv}}^2(\pi f_0) - m_{a_1}^2 + im_{a_1} \Gamma_{a_1}} (C_1^c g_{\bar{K}^* K a_1})(C_2^c g) \vec{p}'_{\pi^-} \cdot \vec{k} \times \tilde{t}_T(m_{K^{*+}}, m_{\bar{K}^0}, m_{K^0})(t_{\bar{K}^0 K^0 \rightarrow \pi^+ \pi^-}).
 \end{aligned} \tag{32}$$

III. RESULTS

With the former formula Eq. (24), by fixing the value of M_{f_0} , the distributions of the triangle amplitudes \tilde{t}_T , $\text{Im}(\tilde{t}_T)$, $\text{Re}(\tilde{t}_T)$ and $|\tilde{t}_T|^2 \times 1.3 \times 10^7$ as functions of the $M_{\text{inv}}(\pi f_0)$ invariant mass have been shown in Fig. 3 for the $K^{*0} K^+ K^-$ triangle loop diagram. From the Fig. 3, we see that there is a peak around 1418 MeV for the $|\tilde{t}_T|^2$, which is consistent with the result of Eq. (2). Since kinematic factors are the function of the invariant mass $M_{\text{inv}}(\pi f_0)$, as $M_{\text{inv}}(\pi f_0)$ increases, it could impose restrictions on phase space and change the shape of the final mass distribution. According to Ref. [14], we need to consider whether the cutoff q_{max} and triangle singularity will affect the behavior of $\text{Im}(\tilde{t}_T)$. Comparing the three subfigures of Fig. 3 where $M_{\text{inv}}(\pi f_0)$ is fixed at 600, 700, and 800 MeV, respectively, one can find that as the q_{max} increases the behavior of the $\text{Im}(\tilde{t}_T)$ at the higher $M_{\text{inv}}(\pi f_0)$ becomes softer, while the peak that associated to the triangle singularity remains. There are two peaks for $\text{Im}(\tilde{t}_T)$ and $\text{Re}(\tilde{t}_T)$ located at 1440 MeV and 1390 MeV, respectively. The reason is that the peak of $\text{Im}(\tilde{t}_T)$ is derived from the triangle singularity while the peak of $\text{Re}(\tilde{t}_T)$ is derived from the threshold of the $K^{*0} K^\pm$ that is about 1390 MeV in Fig. 1(a). Next, we will more intuitively show the behavior of $\text{Im}(\tilde{t}_T)$ and $\text{Re}(\tilde{t}_T)$ peaks.

In Fig. 4, analogy to Ref. [14], we show the development of triangle singularity of $K^{*0} K^+ K^-$ triangle loop

with $\Gamma_{K^*}/2$ and ϵ fixed at different finite values but close to zero. To reach the triangle singularity in the Fig. 1(a), it is required that the mass of f_0 should be slightly larger than the $K^- K^+$ threshold as in Eq. (1). In Fig. 4, we have taken $m_{f_0} = 990$ MeV. Due to the different sources of the two peaks of $\text{Im}(\tilde{t}_T)$ and $\text{Re}(\tilde{t}_T)$, from Fig. 4, we can see that there are two different distribution behavior for $\text{Re}(\tilde{t}_T)$ and $\text{Im}(\tilde{t}_T)$. For the $\text{Re}(\tilde{t}_T)$, in Fig. 4(a), there is a cusp located at threshold of the $K^{*0} K$ system 1390 MeV and a sharp downfall nearby the triangle singularity 1418 MeV. And, in Fig. 4(b), the triangle singularity appears in the form of narrow peak around 1418 MeV in the distribution of $\text{Im}(\tilde{t}_T)$. At the same time, by taking the different values of $\Gamma_{K^*}/2$ and ϵ , namely 1, 0.5, 0.25, and 0.1 MeV, Fig. 4 shows that as the values decreases, the cusp of the $\text{Re}(\tilde{t}_T)$ converges to a finite value, which is associated to the threshold of the $K^{*0} K$, and the peak of $\text{Im}(\tilde{t}_T)$ becomes more and more sharp and finally transforms into a singularity when $\Gamma_{K^*}/2 = \epsilon = 0$.

As shown in Fig. 5(a), differential distributions of decay width Γ' have been depicted for different $f_0(980)$ masses $M_{f_0} = 980, 983, \text{ and } 987$ MeV. It is clear that the mass of $f_0(980)$ will enhance the result of decay width, but the peaks of differential distributions are still located around the location of the triangle singularity $M_{\text{inv}}(\pi f_0) = 1418$ MeV. In Fig. 5(b), we plot the double differential

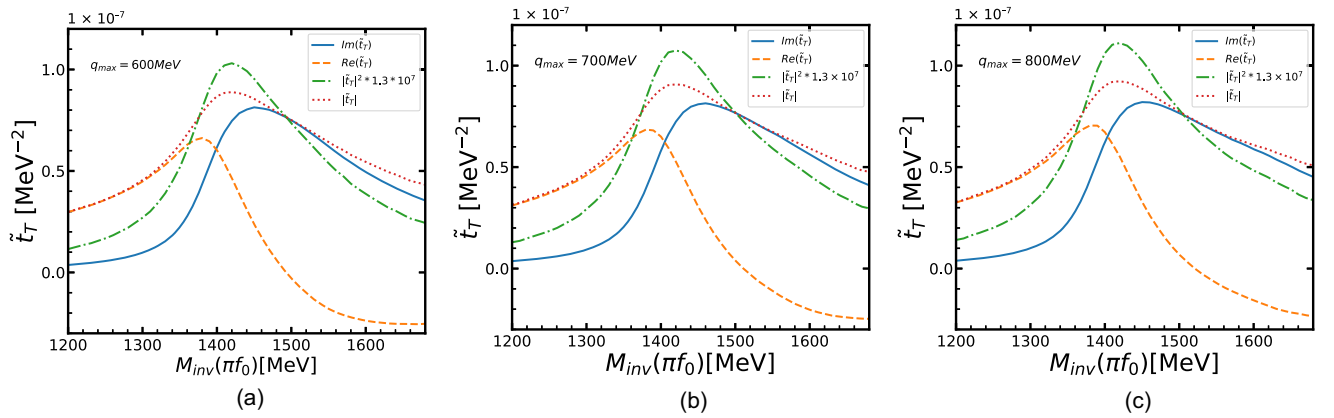


FIG. 3. The distributions of the triangle amplitude \tilde{t}_T for the $K^{*0} K^+ K^-$ triangle loop in the Fig. 1(a). We take $M_{f_0} = 980$ MeV, and times 1.3×10^7 for t_T^2 .

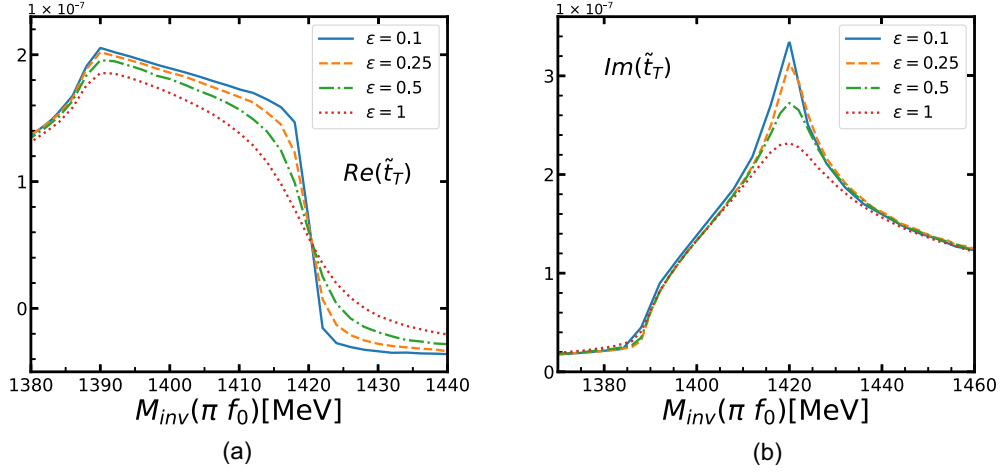


FIG. 4. The distributions of the real (a) and imaginary (b) parts of \tilde{t}_T for the $K^{*0}K^+K^-$ triangle loop by taking $M_{f_0} = 990$ MeV and the different values of $\Gamma_{K^*}/2 = \epsilon = 1, 0.5, 0.25,$ and 0.1 MeV.

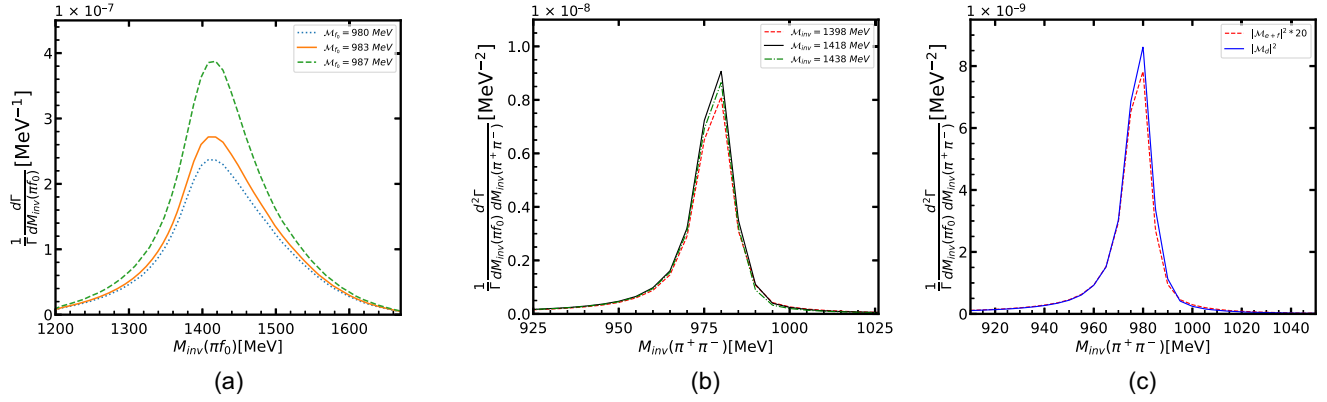


FIG. 5. (a) The differential distribution of decay width Γ' for $f_0(980)$ productions, as Eq. (25). (b) The double differential distribution of decay width Γ as a function of the invariant mass $M_{\text{inv}}(\pi^+\pi^-)$ for the four body decay processes at $M_{\text{inv}}(\pi f_0) = 1398, 1418$ and 1438 MeV. (c) The differential distributions of Γ for Figs. 1(d) and 1(e) plus Fig. 1(f) with $M_{\text{inv}}(\pi f_0) = 1418$ MeV.

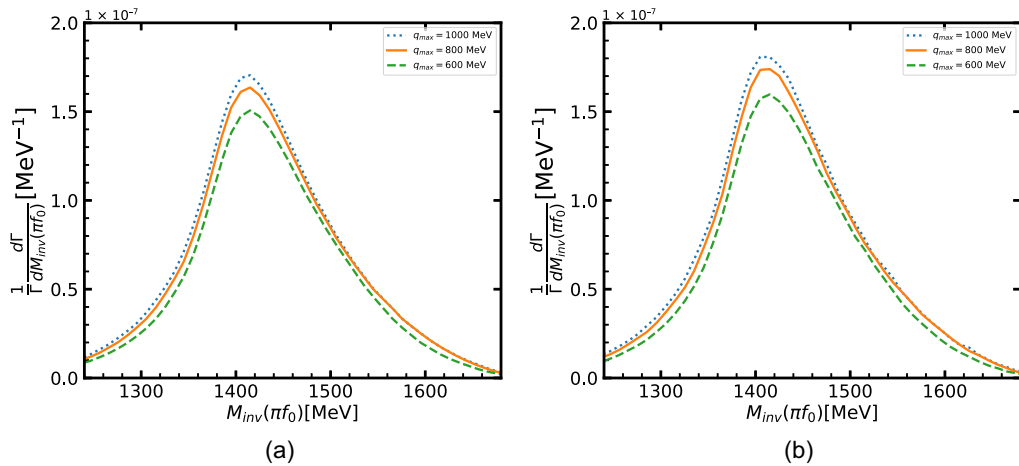


FIG. 6. The differential distribution of decay width Γ as a function of the invariant mass $M_{\pi f_0}$ for the four body decay processes. (a) The integration region is $M_{f_0} \in [900, 1000]$ MeV. (b) The integration region is $M_{f_0} \in [800, 1200]$ MeV.

distribution of decay width $\frac{1}{\Gamma_{D^0}} \frac{d^2\Gamma}{dM_{\text{inv}}(\pi f_0) dM_{\text{inv}}(\pi^-\pi^+)}$ as a function of the invariant mass $M_{\text{inv}}(\pi^-\pi^+)$ in the region of the $f_0(980)$ for the four body decay process. In Fig. 5(b), we take $M_{\text{inv}}(\pi f_0) = 1398, 1418, \text{ and } 1438$ MeV as triangle singularity is around. For the Fig. 5(b), there is a clear peak around the 980 MeV, and have strong contribution to $M_{\text{inv}}(\pi^+\pi^-)$ distribution around the region of $M_{\text{inv}}(\pi^+\pi^-) = 980$ MeV. The Fig. 5(c) shows that although we consider the contributions of the intermediate state a_1 , it is very small compared with the Fig. 1(a). Moreover, the peak at triangle singularity ($M_{\text{inv}}(\pi f_0) = 1418$) is significantly larger than the values of $M_{\text{inv}}(\pi f_0) = 1398$ and 1438 MeV. In the following analysis, we only focus on the domain of $f_0(980)$, and the main contribution comes from the range of $M_{f_0} \in [900, 1000]$. Therefore, we can restrict integral range of $M_{\text{inv}}(\pi^+\pi^-)$ of Eq. (31) to these limits. Further, we can obtain the differential distribution for $\frac{1}{\Gamma_{D^0}} \frac{d\Gamma}{dM_{\text{inv}}(\pi f_0)}$ as a function of the invariant mass $M_{\text{inv}}(\pi f_0)$. The results have been depicted in Fig. 6. From the Fig. 6, for the total contribution, there is a clear peak located at 1418 MeV with considering the $f_0(980)$ as a dynamically generated states, which is consistent with Figs. 3 and 5.

IV. SUMMARY

In the present work, we give the derivation details and formalism for the decay width calculation of $D^0 \rightarrow \pi^+\pi^-f_0(980)$, $f_0 \rightarrow \pi^+\pi^-$ process. From the Fig. 1(a), D^0 first decays to $K^{*0}\pi K$, then the K^{*0} decays to the $\pi\bar{K}$ and the $\bar{K}K$ fuse to form a $f_0(980)$. Only the triangle mechanism corresponding to $K^{*0}K\bar{K}$ triangle diagrams can produce triangle singularity around 1418 MeV for the invariant mass of $M_{\text{inv}}(\pi f_0)$. Through calculating the $\frac{d^2\Gamma}{dM_{\text{inv}}(\pi f_0) dM_{\text{inv}}(\pi^+\pi^-)}$, a clear peak is produced in the invariant mass distribution of $\pi^+\pi^-$ system that comes from the f_0 decay, showing a clear $f_0(980)$ shape. After integrating over $M_{\text{inv}}(\pi^+\pi^-)$, the $\frac{d\Gamma}{dM_{\text{inv}}(\pi f_0)}$ shows a clear peak in the $M_{\text{inv}}(\pi f_0)$ invariant mass distribution located at 1418 MeV, and the main contribution of the peak comes from the triangle singularity.

ACKNOWLEDGMENTS

The authors thank professor Weihong Liang and professor Eulogio Oset for their patient guidance. H. S. is supported by the National Natural Science Foundation of China (Grants No. 12075043, No. 12147205).

-
- [1] R. F. Peierls, *Phys. Rev. Lett.* **6**, 641 (1961).
 - [2] I. J. R. Aitchison, *Phys. Rev.* **133**, B1257 (1964).
 - [3] J. B. Bronzan, *Phys. Rev.* **134**, B687 (1964).
 - [4] S. Coleman and R. E. Norton, *Nuovo Cimento* **38**, 438 (1965).
 - [5] R. Karplus, C. M. Sommerfield, and E. H. Wichmann, *Phys. Rev.* **111**, 1187 (1958).
 - [6] L. Landau, *Nucl. Phys.* **13**, 181 (1960).
 - [7] J.-J. Wu, X.-H. Liu, Q. Zhao, and B.-S. Zou, *Phys. Rev. Lett.* **108**, 081803 (2012).
 - [8] F. Aceti, W. H. Liang, E. Oset, J. J. Wu, and B. S. Zou, *Phys. Rev. D* **86**, 114007 (2012).
 - [9] X.-G. Wu, J.-J. Wu, Q. Zhao, and B.-S. Zou, *Phys. Rev. D* **87**, 014023 (2013).
 - [10] N. N. Achasov, A. A. Kozhevnikov, and G. N. Shestakov, *Phys. Rev. D* **92**, 036003 (2015).
 - [11] N. N. Achasov and G. N. Shestakov, *Pis'ma Zh. Eksp. Teor. Fiz.* **107**, 292 (2018) [*JETP Lett.* **107**, 276 (2018)].
 - [12] F. Aceti, J. Dias, and E. Oset, *Eur. Phys. J. A* **51**, 48 (2015).
 - [13] N. N. Achasov, A. A. Kozhevnikov, and G. N. Shestakov, *Phys. Rev. D* **93**, 114027 (2016).
 - [14] R. Pavao, S. Sakai, and E. Oset, *Eur. Phys. J. C* **77**, 599 (2017).
 - [15] F. Aceti, L. R. Dai, and E. Oset, *Phys. Rev. D* **94**, 096015 (2016).
 - [16] S. Sakai, E. Oset, and W. H. Liang, *Phys. Rev. D* **96**, 074025 (2017).
 - [17] W.-H. Liang, S. Sakai, J.-J. Xie, and E. Oset, *Chin. Phys. C* **42**, 044101 (2018).
 - [18] M. Mikhasenko, B. Ketzer, and A. Sarantsev, *Phys. Rev. D* **91**, 094015 (2015).
 - [19] L. R. Dai, Q. X. Yu, and E. Oset, *Phys. Rev. D* **99**, 016021 (2019).
 - [20] A. Feijoo, R. Molina, L. R. Dai, and E. Oset, *Eur. Phys. J. C* **82**, 1028 (2022).
 - [21] Y. Yu, Y.-K. Hsiao, and B.-C. Ke, *Eur. Phys. J. C* **81**, 1093 (2021).
 - [22] Q. Huang and J.-J. Wu, *Phys. Rev. D* **104**, 116003 (2021).
 - [23] J.-J. Xie, L.-S. Geng, and E. Oset, *Phys. Rev. D* **95**, 034004 (2017).
 - [24] Y. Huang, M.-Z. Liu, J.-X. Lu, J.-J. Xie, and L.-S. Geng, *Phys. Rev. D* **98**, 076012 (2018).
 - [25] L. Roca and E. Oset, *Phys. Rev. C* **95**, 065211 (2017).
 - [26] V. R. Debastiani, S. Sakai, and E. Oset, *Phys. Rev. C* **96**, 025201 (2017).
 - [27] D. Samart, W.-h. Liang, and E. Oset, *Phys. Rev. C* **96**, 035202 (2017).
 - [28] S. Sakai, E. Oset, and A. Ramos, *Eur. Phys. J. A* **54**, 10 (2018).
 - [29] J.-J. Xie and F.-K. Guo, *Phys. Lett. B* **774**, 108 (2017).
 - [30] M. Bayar, R. Pavao, S. Sakai, and E. Oset, *Phys. Rev. C* **97**, 035203 (2018).

- [31] X.-H. Liu, M. Oka, and Q. Zhao, *Phys. Lett. B* **753**, 297 (2016).
- [32] L. R. Dai, R. Pavao, S. Sakai, and E. Oset, *Phys. Rev. D* **97**, 116004 (2018).
- [33] J.-J. Xie and E. Oset, *Phys. Lett. B* **792**, 450 (2019).
- [34] W.-H. Liang, H.-X. Chen, E. Oset, and E. Wang, *Eur. Phys. J. C* **79**, 411 (2019).
- [35] X.-H. Liu, G. Li, J.-J. Xie, and Q. Zhao, *Phys. Rev. D* **100**, 054006 (2019).
- [36] J.-J. Xie, G. Li, and X.-H. Liu, *Chin. Phys. C* **44**, 114104 (2020).
- [37] H.-J. Jing, S. Sakai, F.-K. Guo, and B.-S. Zou, *Phys. Rev. D* **100**, 114010 (2019).
- [38] S. X. Nakamura, *Phys. Rev. D* **102**, 074004 (2020).
- [39] S. Sakai, *Phys. Rev. D* **101**, 074041 (2020).
- [40] X.-Z. Ling, M.-Z. Liu, J.-X. Lu, L.-S. Geng, and J.-J. Xie, *Phys. Rev. D* **103**, 116016 (2021).
- [41] R. Molina and E. Oset, *Eur. Phys. J. C* **80**, 451 (2020).
- [42] E. Wang, J.-J. Xie, W.-H. Liang, F.-K. Guo, and E. Oset, *Phys. Rev. C* **95**, 015205 (2017).
- [43] Y.-K. Hsiao, Y. Yu, and B.-C. Ke, *Eur. Phys. J. C* **80**, 895 (2020).
- [44] S. Sakai, E. Oset, and F.-K. Guo, *Phys. Rev. D* **101**, 054030 (2020).
- [45] V. R. Debastiani, S. Sakai, and E. Oset, *Eur. Phys. J. C* **79**, 69 (2019).
- [46] E. Oset and L. Roca, *Phys. Lett. B* **782**, 332 (2018).
- [47] Z.-M. Ding, H.-Y. Jiang, and J. He, *Eur. Phys. J. C* **80**, 1179 (2020).
- [48] L. R. Dai, L. Roca, and E. Oset, *Phys. Rev. D* **99**, 096003 (2019).
- [49] Y. Huang, J.-X. Lu, J.-J. Xie, and L.-S. Geng, *Eur. Phys. J. C* **80**, 973 (2020).
- [50] Y. Huang, C.-j. Xiao, Q. F. Lü, R. Wang, J. He, and L. Geng, *Phys. Rev. D* **97**, 094013 (2018).
- [51] W. H. Liang and E. Oset, *Phys. Lett. B* **737**, 70 (2014).
- [52] J. A. Oller and E. Oset, *Nucl. Phys.* **A620**, 438 (1997); **A652**, 407(E) (1999).
- [53] J. A. Oller, E. Oset, and J. R. Pelaez, *Phys. Rev. D* **59**, 074001 (1999); **60**, 099906(E) (1999); **75**, 099903(E) (2007).
- [54] M. Bayar, F. Aceti, F.-K. Guo, and E. Oset, *Phys. Rev. D* **94**, 074039 (2016).
- [55] F.-K. Guo, X.-H. Liu, and S. Sakai, *Prog. Part. Nucl. Phys.* **112**, 103757 (2020).
- [56] P. Zyla *et al.* (Particle Data Group), *Prog. Theor. Exp. Phys.* **2020**, 083C01 (2020).
- [57] W. Wang and Z.-X. Zhao, *Eur. Phys. J. C* **76**, 59 (2016).
- [58] R. Molina, M. Doering, W. H. Liang, and E. Oset, *Eur. Phys. J. C* **81**, 782 (2021).
- [59] S. Scherer, *Adv. Nucl. Phys.* **27**, 277 (2003).
- [60] A. Pich, *Rep. Prog. Phys.* **58**, 563 (1995).
- [61] L. Roca, E. Oset, and J. Singh, *Phys. Rev. D* **72**, 014002 (2005).
- [62] J. M. Link *et al.* (FOCUS Collaboration), *Phys. Rev. D* **75**, 052003 (2007).